DESIGN TECHNIQUES FOR HIGH BY-PASS RATIO POWERPLANT NOZZLE SYSTEMS

A. R. Seed
National Gas Turbine Establishment
Pyestock, Farnborough, Hampshire, UK

Abstract

Theoretical and experimental techniques used to identify and prove high efficiency gas generator afterbodies for high by-pass ratio turbofan installations are outlined. The theoretical method of characteristics is used to predict afterbody flows on axisymmetric afterbodies. The value of this method in predicting 'shock free' flows is demonstrated. A model technique giving accurate comparisons between a range of axisymmetric isolated nozzle arrangements up to high subsonic Mach numbers is described. Results are presented which demonstrate the accuracy and repeatability of the model technique, and the applicability of the theoretical and experimental approaches to identifying improved afterbody designs.

I. Introduction

High by-pass ratio turbofan aero engines are now established as the most efficient powerplants for high subsonic Mach No. cruise aircraft. A critical factor in achieving high efficiency has been the minimisation of installation losses associated with the air intake and nozzle systems. In cruising flight, even small improvements to the exhaust system efficiency can be highly rewarding by virtue of the large ratio of gross to net thrust associated with a low specific thrust engine. An area of particular concern on short fan cowl arrangements is the development of the flow from the fan nozzle over the gas generator afterbody where at typical cruise conditions the annular jet is at supercritical pressure ratio.

The early development of gas generator afterbody arrangements was principally based on experimental work, with only empirical allowance for theoretical effects. This paper discusses the application of a simplified theoretical approach to afterbody design. The experimental techniques used at NGTE to investigate design improvements are described. Results are presented which demonstrate the effectiveness of the theoretical and experimental techniques in effecting a significant improvement to an established design.

II. Theoretical analysis

At high subsonic Mach No. cruise conditions, the combination of aircraft dynamic head with the subcritical pressure rise across the fan of a high by-pass ratio engine results in the flow from the fan nozzle being supercritical (typically 2.4 to 2.7 fan nozzle expansion ratio on engines such as RB211, CF6 and JT9D).

In Reference 1 Street has proposed the method of characteristics for the calculation of the flow field over the gas generator afterbody, covering two dimensional and axisymmetric bodies. In this method, the inner boundary is specified by the afterbody profile, and the outer boundary by pressure distribution which has been limited to the constant pressure associated with zero free stream Mach No. This method has been extended by Young[2], to include computation of the flow field external to the powerplant. Although the method, in both cases, has proved of great value in assessing early afterbody profiles prior to experimental test, it has not proved amenable for the generation of high efficiency afterbodies. The method of Reference 1 was therefore modified by the addition of an alternative inner boundary condition; namely, specification of an inner boundary pressure distribution.

Referring to Figure 1, the starting and boundary conditions are specified by:

(a) An initial sonic line described by fan nozzle inner and outer dimensions and inclination to the axial direction. The initial line has been assumed to be linear.

(b) The inner boundary, shown in Figure 1, is defined by:
Initial radius or height given by fan nozzle inner exit dimension.
Initial slope, θ_o, relative to axial direction.
Specified axial surface static distribution with sonic conditions at the fan nozzle exit.

(c) The outer boundary is specified as in Reference 1 to start at the outer fan nozzle dimension and thereafter by constant ambient static pressure.

Two major assumptions built into Reference 1 have been retained, namely the treatment afforded the occurrence of shock waves, and the appearance of localised subsonic flow regions.

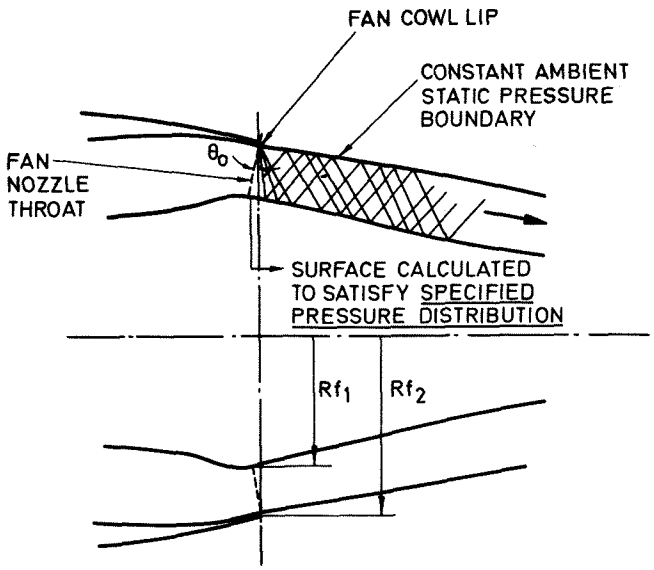

Figure 1. Start and Boundary Conditions

Shock waves

The proper treatment of shock waves, as manifest by intersections of characteristics of the same family, is not included. When such intersections occur, the upstream characteristic is deleted and the downstream characteristic allowed to continue with increased strength. Entropy is assumed unchanged across the shock. The assumption is justified on the basis that:

(a) The method is aimed at generating afterbody profiles which are shock free.

(b) Where shocks do occur these tend to be of oblique form and are limited to the outer flow region as shown in Figure 2(a). Figure 2(b) shows the calculated characteristics network where the occurrence of characteristic intersections is confined to the outer flow region.

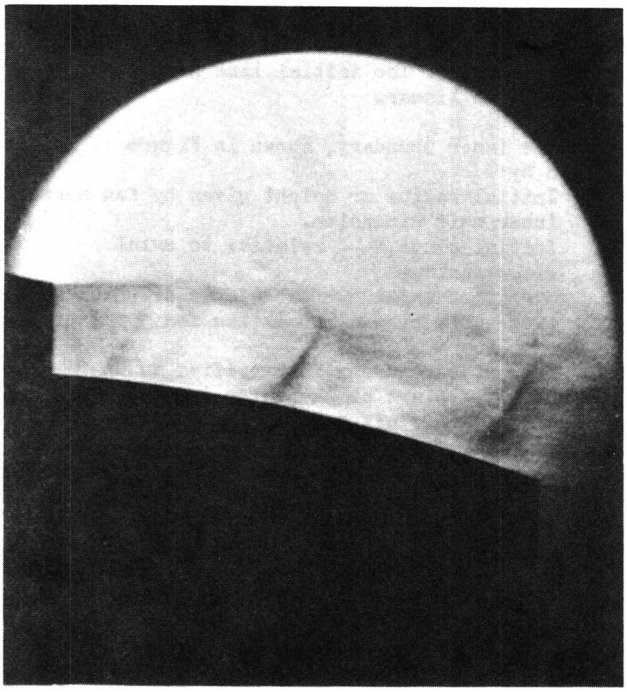

Figure 2(a). Experimental Flow Development

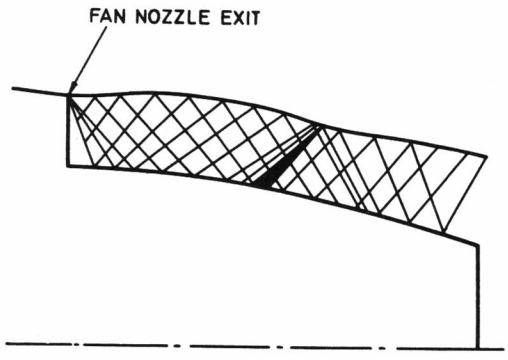

Figure 2(b). Calculated Flow Development

Subsonic flow regions

These can occur on the surface immediately following a rapid compression as indicated in Figure 2(b). Where such subsonic regions are small, as with profiles free of rapid compression processes, the Mach No. is 'forced' to remain slightly supersonic in the region.

III. Application of theory to afterbody design

The design of the most suitable afterbody for an axisymmetric short fan cowl high by-pass powerplant is, typically, bounded by the following set of constraints:

Fan nozzle exit area,
Internal and external radii of fan nozzle annulus,
Gas generator nozzle area and diameter.

The variables considered here which are available to the afterbody designer are:

(a) The angle by which the flow leaving the fan nozzle is tilted towards the axis, θ_o,

(b) The axial variation of afterbody surface static pressure,

(c) The afterbody length.

Since the method does not work to a prescribed final afterbody radius, the evolution of the afterbody profile which meets all the above boundary conditions is an iterative process.

Several distinctive features characterised the afterbody profiles originally specified for the large fan engines (JT9D, RB211, CF6). From Figure 3, these are:

1. direction of flow leaving fan nozzle is close to axial;

2. high inwards flow deflection exerted by the afterbody (RB211, CF6);

3. provision of plug nozzle to enlarge primary nozzle external diameter, hence reducing need to deflect flow inwards around afterbody.

The fan nozzle flow development over a relatively short highly curved afterbody is typified in Figure 4(a) by large over expansion regions to high supersonic Mach No. followed by strong compression regions with shock wave formation in alternating patterns. Towards the trailing edge of the afterbody, a significant region of flow separation can develop. Theoretical analysis of this flow showed that the initial expansion to a highly overexpanded supersonic Mach No. results mainly from the high curvature of the afterbody in this region as indicated in Figure 4. The use of a longer afterbody to reduce the external curvature, also shown in Figure 4, although effective in reducing maximum surface velocities can lead to increased skin friction drag.

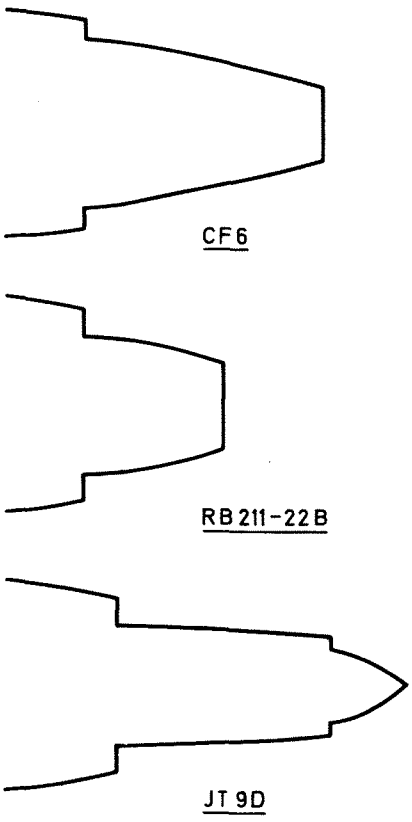

Figure 3. Large Fan Engines - Original Nozzle Arrangements

In applying the theoretical method to design improved efficiency afterbodies, the two surface Mach No. distributions shown in Figure 5(a) emerged as those offering potential for a realistic improvement. In distribution (1) the flow has been expanded quickly to the fully expanded free stream value where it is held constant over the length of the afterbody. Pattern (2) shows a mild over-expansion followed by a slow re-compression to a pressure above free stream ambient which is held constant over the final part of the afterbody. Applying pattern (1) to a typical cruise condition (for EPR = 2.5) the effect of flow turning within the fan nozzle (θ_0) is shown in Figure 5(b) to lead to shortening of the afterbody length proportionally as θ_0 is increased. The afterbody profile associated with pattern (2) is shown, also in Figure 5(b), to be somewhat similar to pattern (1) profiles over the early portion of the afterbody, the major difference appearing towards the trailing edge where the profile turns back towards the axial direction.

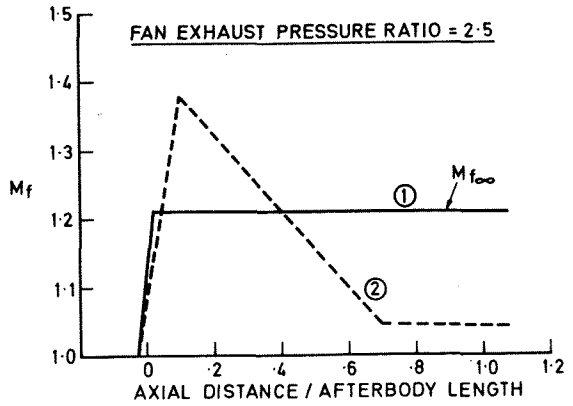

Figure 5(a). Specified Afterbody Surface Mach No. Axial Distributions

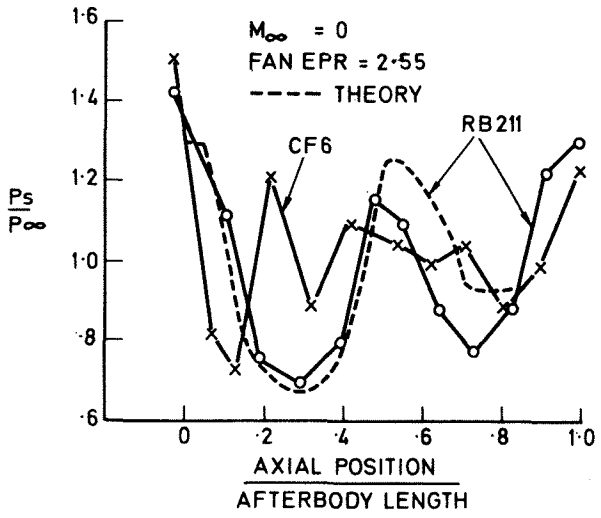

Figure 4. Experimental and Theoretical Afterbody Flows

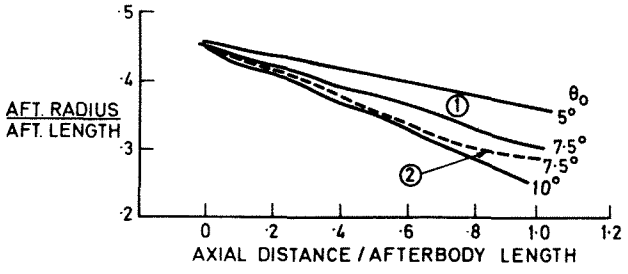

Figure 5(b). Calculated Afterbody Profiles

These calculated profiles are characterised by recurring waviness; however, a major feature is the near linearity of the mean line around which the profile oscillates. Figure 6 shows, over a range of fan nozzle exhaust pressure ratios, that, although the amplitude and wavelength vary, the linearity and angle of the mean line remain substantially constant. Experimental investigation of a linear profile which in an axisymmetric powerplant leads to a conical afterbody was therefore considered to be well worthwhile for the reasons that:

1. it is a simple geometric shape to manufacture;

2. the effect of boundary layer growth will produce a displacement profile tending towards profile (2) in Figure 5(b) so providing the pressure field needed to recover the sin θ_0 term of stream momentum at the fan nozzle exit.

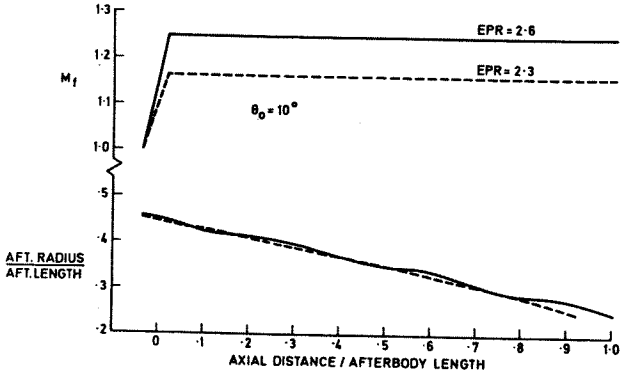

Figure 6. Effect of Fan Exhaust Pressure Ratio

Figure 7 shows the computed and measured pressure distributions for a 10° conical afterbody. Comparison with the measured pressure distribution of the highly curved profile of Figure 3 shows a significant reduction in maximum surface Mach No.

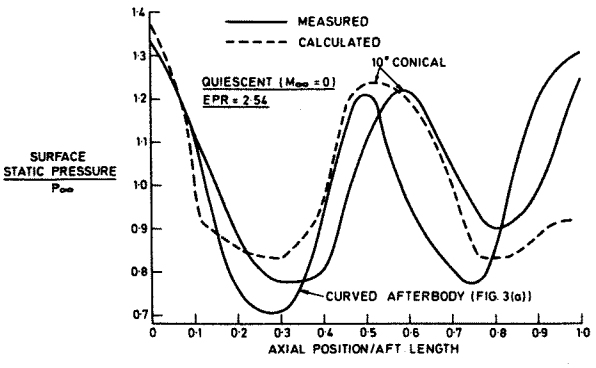

Figure 7. Afterbody Pressure Distributions, Calculated and Measured

IV. Model test techniques

Test rig and model arrangement

The main test facility for the evaluation of two stream nozzle system performance incorporates very accurate measurements of thrust and air mass flows to the two streams. The rig, shown schematically in Figure 8, can simulate the full flight speed range of a subsonic aircraft and although most research activity involves axisymmetric models, can handle non-symmetric models. The techniques used to ensure accuracy of both air flow and thrust measurement are basically those described in Reference 3, but updated by the use of a sensitive and accurate electrical load cell in the thrust meter. The test model is mounted in a slotted octagonal wind tunnel by means of a central upstream sting arrangement. The tunnel operates at ambient stagnation conditions, with the air being induced via the bellmouth shown in Figure 8(a). By using an octagonal tunnel section, based on Reference 4, it has been possible to include flat optical windows to provide high quality Schlieren pictures of the developing flow from the fan nozzle.

For operation in the quiescent mode (Figure 8(b)) the bellmouth intake is replaced by a seal plate which fits closely to the sting, but does not touch it. The tunnel suction section is replaced by a diffuser through which the exhaust air is discharged to atmosphere.

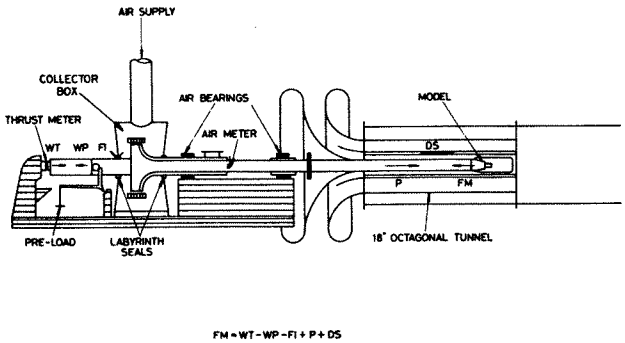

Figure 8(a). Thrust Rig in Wind Tunnel

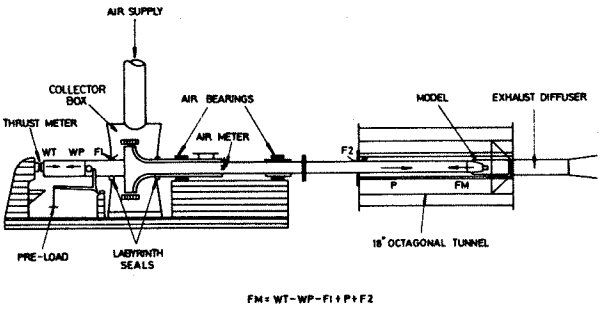

Figure 8(b). Thrust Rig Configured for Quiescent Testing

A typical model arrangement is shown in Figure 9. The model force measurement on the rig balance includes the stream momentum terms associated with the primary and by-pass nozzle systems and the drag forces acting on the fan cowl external surface.

Model scale is typically 1/22 nd of RB211 and at the cruise conditions of 0.85 Mn at 35,000 ft Reynolds No. is about 1/6 th of full scale.

Tunnel blockage imposed by this model is 6.25 per cent with zero nozzle flow, and with the nozzle system just choked blockage is typically 3.5 per cent.

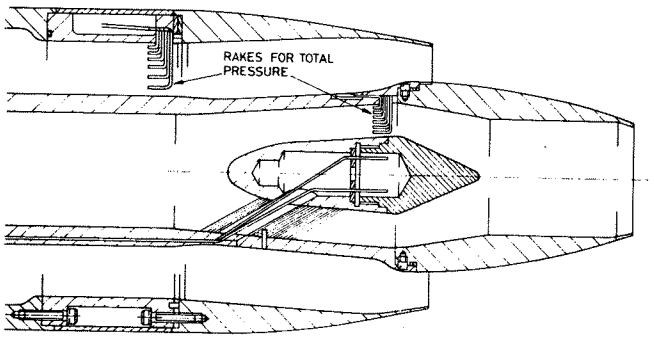

Figure 9. Layout of the Model

Rig and model calibrations

Model exhaust system performance is assessed as the ratio of actual gross thrust minus drag to ideal thrust in the form, F_M/F_{ID}, where

$$\frac{F_M}{F_{ID}} = \frac{\text{Actual thrust developed for a given applied pressure ratio less fan cowl external drag}}{\text{sum of the ideal convergent thrusts of the fan and primary nozzles exhausting separately to freestream static pressure}}$$

Actual thrust minus drag

The accurate determination of the measured quantities has been a fundamental aim of the rig design, necessitating careful design both to minimise extraneous forces and to achieve consistent day-to-day readings. Reference to Figure 8 shows that the measured model force is derived indirectly by correcting the thrust meter load to allow for forces arising from:

air leakage at the seals between collector box and sting, and
tunnel seal plate (at quiescent flight condition);
sting drag (in forward flight);
axial pressure force on sting arising from difference between tunnel total pressure at front and tunnel static at rear

A crucial part of the rig development has been the careful calibration of these terms.

Ideal convergent thrust

Taking two convergent nozzles exhausting separately to free stream static pressure, the ideal convergent thrust is given by:

(i) both nozzles critical or supercritical

$$F_{ID} = Q_p V_p^* + A_p^* (P_{ep}^* - P_\infty) + Q_f V_f^* + A_f^* (P_{ef}^* - P_\infty) \quad \ldots\ (1)$$

where, Q is mass flow rate
V*, A*, P* are throat velocity, area, pressure referred to sonic conditions
suffix p refers to primary nozzle
suffix f refers to fan nozzle
suffix e refers to nozzle exit plane
suffix ∞ refers to free stream at infinity

(ii) both nozzles subcritical

$$F_{ID} = Q_p V_p + Q_f V_f \quad \ldots\ (2)$$

Where one stream is supercritical and the other subcritical the relevant relationships are applied to each stream.

The mass flow values used are those measured, while the velocity terms are based on pressure readings.

Mass flow

Total mass flow measurement is provided by the rig airmeter which was calibrated against a standard NGTE nozzle of known vacuum thrust efficiency by the method of Reference 5.

In deriving the primary nozzle mass flow (Q_p) two methods have been developed,

(i) the primary nozzle flow calibration is obtained from a standard flow measuring rig[5];

(ii) the use of a rake derived total pressure measurement together with a static pressure measurement and a knowledge of flow area in the same plane allows the derivation of $Q_p \sqrt{T}$.

With primary nozzle applied pressure ratios often only just supercritical, the derivation of mass flow is not considered to be fully satisfactory, however small inaccuracies in primary flow measurement do not cause a significant error in the ideal convergent thrust since

(a) primary mass flow is about 25 per cent of the total flow so that, typically a 1 per cent error in Q_p appears as a $\frac{1}{4}$ per cent error in $Q_p + Q_f$.

(b) With fan and primary exhaust pressure ratios fairly close, errors in Q_p are largely compensated by the associated error generated in Q_f, since

$$Q_f = Q_{airmeter} - Q_p$$

Pressure measurement pressures

Rake derived total pressures, using the rakes shown in Figure 9, are used for both primary and by-pass streams.

Freestream static pressure

The reference freestream static pressure has been taken in a region where the axial distribution of tunnel wall-pressure is, relatively, both constant and unaffected by nozzle build changes and blowing conditions. Figure 10 shows the axial distribution of Mach No. at the tunnel wall based on the static measurement at working section X/L = 0.85.

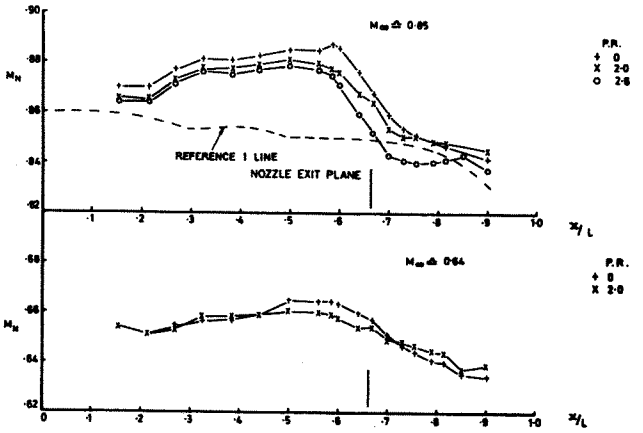

Figure 10. Axial Mach Number Distributions at Tunnel Wall

Accuracy and repeatability

A major aim in the development of this model testing technique has been the achievement of a high degree of both accuracy and repeatability of results. High accuracy is taken to be synonymous with the minimisation of systematic errors. Repeatability refers to the scatter of points which results from random errors.

Under external flow conditions, a source of systematic error is that associated with the relatively high model blockage in the tunnel. The attainment of high absolute accuracy from such a rig is the subject of a continuing study[6]. By careful calibration and use of the rig, however, it is believed that comparative testing of different nozzle arrangements can be carried out with a high degree of confidence.

The effectiveness of techniques aimed at minimising scatter and the achievement of good repeatability is indicated in Figure 11 which shows thrust performance test data taken on separate occasions. The maximum scatter about the mean line is within ±0.2 per cent of F_M/F_{ID}.

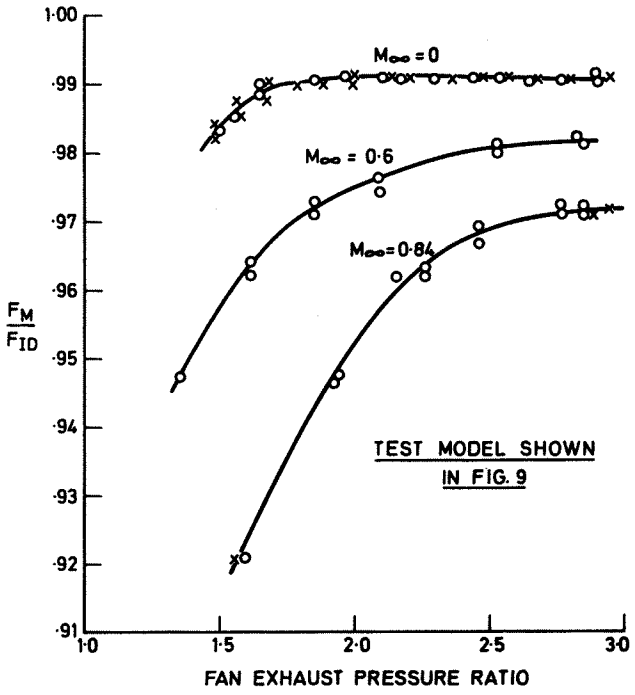

Figure 11. Typical Test Results

V. Experimental evaluation of conical afterbody

Following the theoretical work outlined in Section III, initial investigations were centred around a 10° conical afterbody as shown in Figure 12. A highly curved afterbody selected as the original production geometry for the RB211, Reference 7, is shown superimposed on Figure 12(a). Comparative tests between clean axisymmetric builds of these two afterbodies were conducted using the same fan cowl.

Figure 12(b) shows comparative performance curves at typical cruise flight conditions. The fitted lines through the experimental points show that the 10° afterbody has generated reduced nozzle losses of about 0.3 per cent gross thrust at cruise pressure ratio, equivalent to about 0.75 per cent gain in nett thrust. Figure 13 shows surface static pressure distributions measured on the two afterbodies at both quiescent and cruise Mach No. conditions. Two features of note are:

(a) the minimum surface pressure values of the conical afterbody are somewhat higher than the equivalent curved afterbody values, particularly at the high freestream Mach No. condition;

(b) the changes in pressure distributions from the static to cruise conditions are quite opposite, with the initial low pressure region on the curved afterbody being greatly extended while that on the conical afterbody is much reduced.

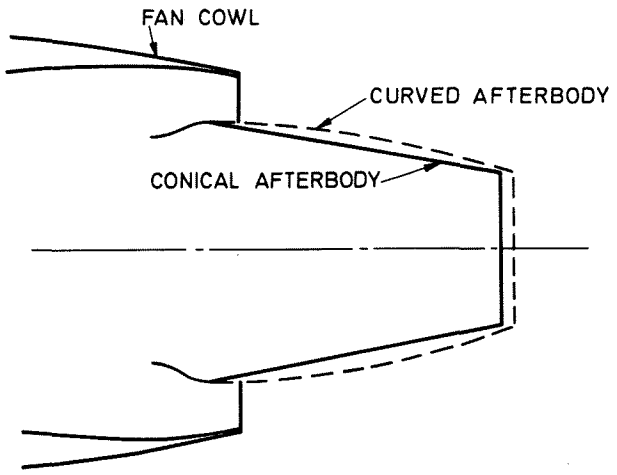

Figure 12(a). Conical Afterbody Test Configuration

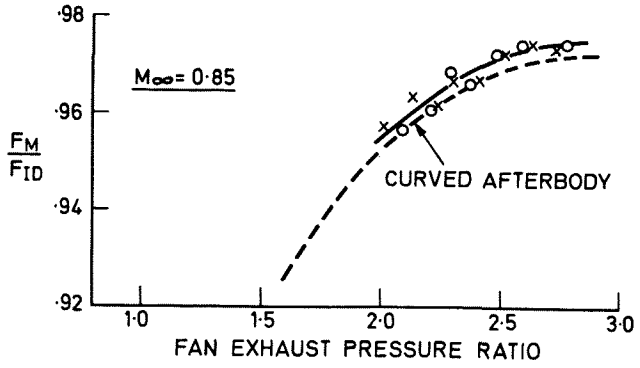

Figure 12(b). 10° Conical Afterbody Performance

Calculation of the skin friction drag values at the cruise condition (M_∞ = 0.85) produces the following figures as a fraction of F_{ID},

Curved afterbody, 0.0079

Conical afterbody, 0.0067

so that

$\frac{\text{skin friction force}}{F_{ID}}$ = 0.0012, equivalent to 0.3 per cent of nett thrust

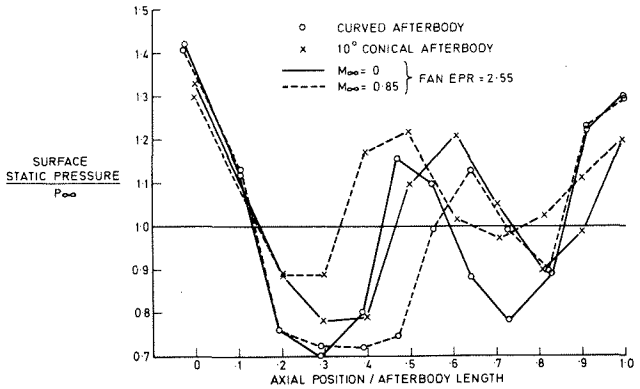

Figure 13. Afterbody Surface Pressure Distributions

Other factors indicated by the pressure distributions, and Schlieren pictures of Figure 14, as contributing to the conical afterbody performance gain are

reduced shock losses resulting from lower fan stream Mach No.;
elimination of the substantial separated flow region which occurs well forward of the trailing edge of the afterbody. This results from a reduced boundary layer growth along the conical afterbody combined with a much reduced compressive flow deflection at the afterbody trailing edge - 10° for the conical as against 19° for the curved afterbody.

The tests described here illustrate the use of the thrust rig for

(i) the determination of optimum high by-pass ratio nozzle systems;

(ii) identification of the factors leading to differences between model builds.

As a result of this theoretical and experimental work indicating the potential performance improvement offered by a conical afterbody, tests on this type of afterbody were carried out independently by the UK engine firm with a view to examining the applicability to the RB211. The Rolls Royce tests, reported in Reference 7, produced a similar result on a 15° conical afterbody which has now been introduced as a production item for the RB211-22B and -524 versions of the engine.

The tests described here constitute part of a continuous programme covering systematic research work into improved nozzle systems for future by-pass engines, alternating with tests on specific project arrangements during definition and development phases.

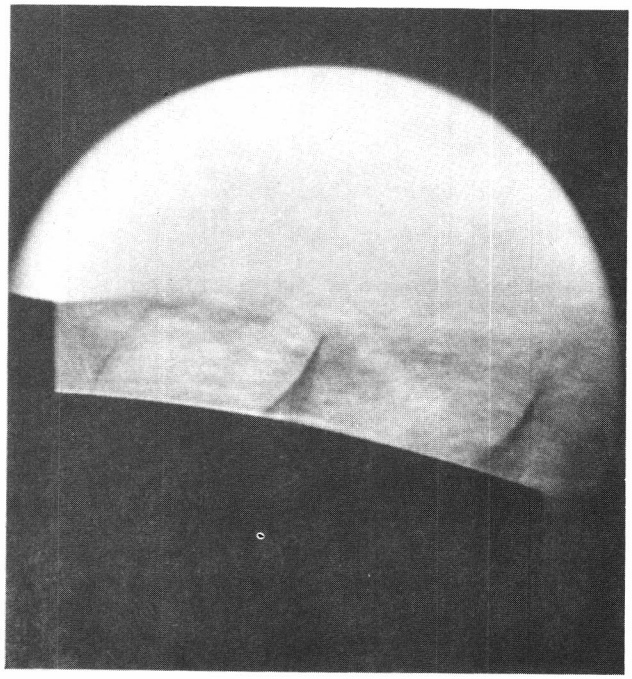

Curved Afterbody
Fan EPR = 2.61

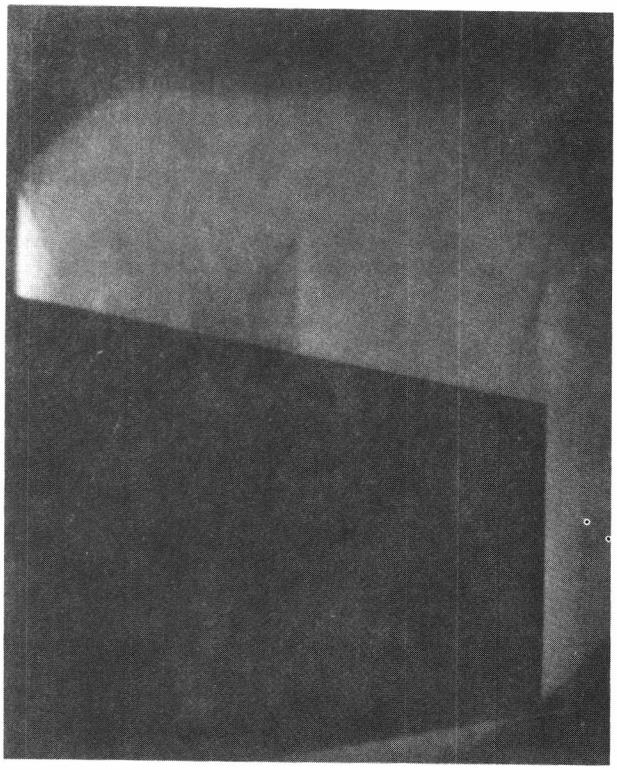

Conical Afterbody

Figure 14. Afterbody Flow Patterns

VI. Conclusions

1. Use of a simplified theoretical model, based on the method of characteristics, has indicated that performance improvements to the gas generator afterbody of a short fan cowl high by-pass powerplant can result from

(a) turning the fan flow radially inwards towards the engine axis prior to the flow leaving the fan nozzle;

(b) use of a simple high angle conical afterbody profile.

2. A thrust rig has been developed to assess the comparative performance of different nozzle arrangements with the inclusion of simulated forward speed up to 0.95 Mach No. By careful calibration and use the high standards of accuracy and consistency needed for the evaluation of small performance increments, which are significant for high by-pass ratio powerplants at cruise, have been achieved.

3. Experimental evaluation of a 10° conical gas generator afterbody derived from the theory showed a worthwhile performance improvement over the more conventional highly curved afterbody. This result, having been validated by independent tests, played a significant part in the adoption of a 15° conical afterbody for production versions of the RB211-22B and RB211-524.

Acknowledgement

The outcome of the work reported here, particularly the design and development of the high accuracy rig, has depended heavily on the efforts of colleagues in the Engine Research Department of NGTE.

References

1. Calculation of the flow field downstream of the fan nozzle of a turbofan aero engine, P G Street, Aeronautical Journal, 74, 983-987, December 1970

2. A theoretical investigation of supersonic jets in subsonic flow fields, C Young, ARC CP 1256, 1973

3. Some experiments on two stream propelling nozzles for supersonic aircraft, W G E Lewis, F W Armstrong, ICAS Paper No. 70-48, 7th Congress, September 1970

4. NASA transonic wind-tunnel test sections, R H Wright, V G Ward, NACA Report 1231, 1955

5. The design point performance of model internal expansion propelling nozzles with area ratios up to 4, M V Herbert, D L Martlew, R A Pinker, ARC R and M 3477, 1967

6. Improved nozzle testing techniques in transonic flow, Edited A Ferri, AGARD-AG-208, October 1975

7. A model technique for exhaust system performance testing, T D Coombes, Paper 17, AGARD-CP-150, September 1974